Enantiomeric Separation of Racemic Drugs Using Chiral Self-Assembled Monolayers

A Major Qualifying Project Report

submitted to the Faculty of

WORCESTER POLYTECHNIC INSTITUTE

in fulfillment of the requirements for the

Degree of Bachelor of Science

by

_____

Thomas Blaisdell

Date: April 29, 2010

Approved:

_____

Professor John C. MacDonald, Advisor

Acknowledgements

I would sincerely like to thank Professor MacDonald for being a supportive and helpful advisor throughout the entirety of this project. Amidst an extremely busy schedule, he was able to meet with me whenever my research had faced an obstacle. I would also like to thank Pranoti Navare for her constant support and patience with my many inquiries. She was a great help and provides me with an ideal template of how a successful and contributing graduate student should function.

Abstract

Enantiomeric separation of racemic drugs is a never ending battle for pharmaceutical chemists. Conventional approaches to separating enantiomers (mirror-image stereoisomers) typically rely on chromatography utilizing chiral stationary phases or reactions of racemic drugs with chiral resolving reagents to form diastereomeric salts that crystallize separately. Separation of enantiomers by those techniques is often difficult and can add significantly to the cost of developing and marketing racemic drugs. The objective of this project was to develop a new surface-based approach to separating enantiomers of racemic drugs via selective crystallization on chiral surfaces consisting of gold substrates functionalized with self-assembled monolayers (SAMs) of a chiral organic compound. We hypothesized that such chiral surfaces would promote diastereomeric interactions with racemates leading (1) to formation of enantiomerically pure crystals (conglomerates) rather than racemic crystals, and (2) to preferential crystallization of one enantiomer in the presence of the other as a means to isolate or enrich the purity of a given enantiomer of a drug. This project builds upon previous work in our lab involving enantiomeric purification of racemic drugs on chiral SAMs of the amino acid cysteine.

Table of Contents

1. Background

1.1 Crystallization

The process of crystallization refers to the formation of a crystalline solid from an evaporating or cooled solution. This phenomenon can be broken down into two stages, namely crystal nucleation and crystal growth.[1,2] Crystal nucleation begins as the concentration of the solute achieves saturation and, eventually, supersaturation through evaporation and/or a reduction of temperature. During this process, molecules begin to cluster together due to favorable intermolecular interactions. Initial formation of aggregates below a certain size is unfavorable because free energy at the surface of the particle outweighs the favorable free energy in the interior of the particle, as shown in the free energy plot shown in Figure 1a. When an aggregate reaches a critical radius, it forms a stable crystal nucleus that defines the packing arrangement and composition of molecules contained with the crystal. Aggregates with sizes below the critical radius are unstable and frequently dissolve. Crystal growth begins when solute molecules add to the surface of a stable crystal nucleus.

There are two different types of nucleation that occur within a supersaturated solution. Homogenous nucleation is when nucleation occurs in the absence of a surface. In this rare instance, it requires very high supersaturation conditions to overcome the free energy of the aggregate. The more common heterogeneous nucleation is nucleation in the presence of a surface. This type lowers the surface energy of the aggregate by binding to it.[3] Figure 1b highlights the process of heterogeneous nucleation.
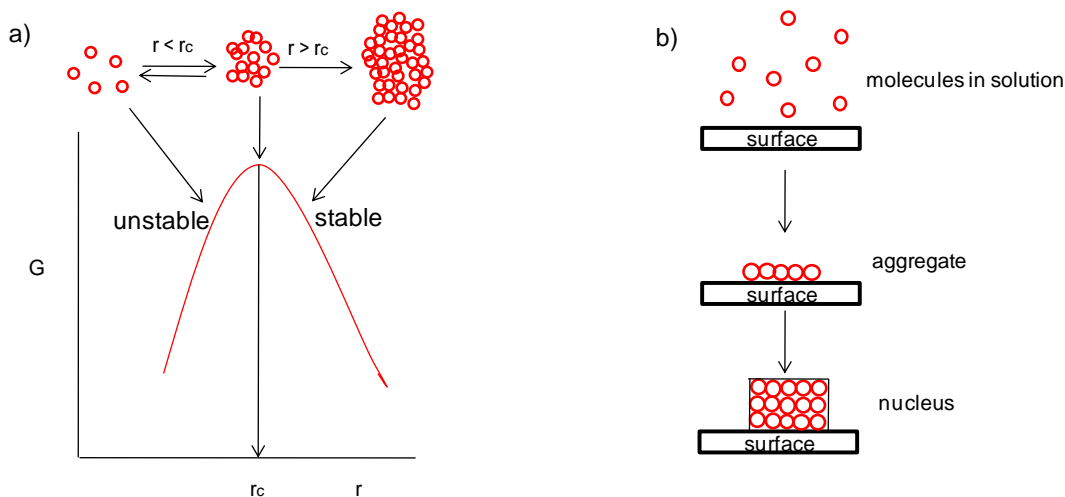
Figure 1: a.) This chart plots free energy (G) with respect to the size of the aggregate (r). At the critical radius (rc), the aggregate forms a stable nucleus and the free energy decreases. b.) This diagram depicts the stepwise process of crystal nucleation on a surface.

1.1.1 Crystallization of racemates

The crystallization of racemic molecules is very similar to the crystallization of achiral molecules. However, because of their chirality, racemic molecules can form different types of crystals with different composition. If both the R and S enantiomers aggregate together then they form a heterochiral racemic crystal with a 1:1 ratio. If the two enantiomers aggregate separately, however, then a homochiral crystal is formed. These enantiomeric pure crystals are called conglomerates. Sometimes, a third type of crystal can be found, called a pseudoracemic crystal. Similar to racemic crystals, pseudoracemic crystals exist in a 1:1 enantiomer ratio. However, in pseudoracemic crystals, the enantiomers pack randomly while racemic crystals pack in an ordered array. These three types of crystals are displayed in Figure 2.
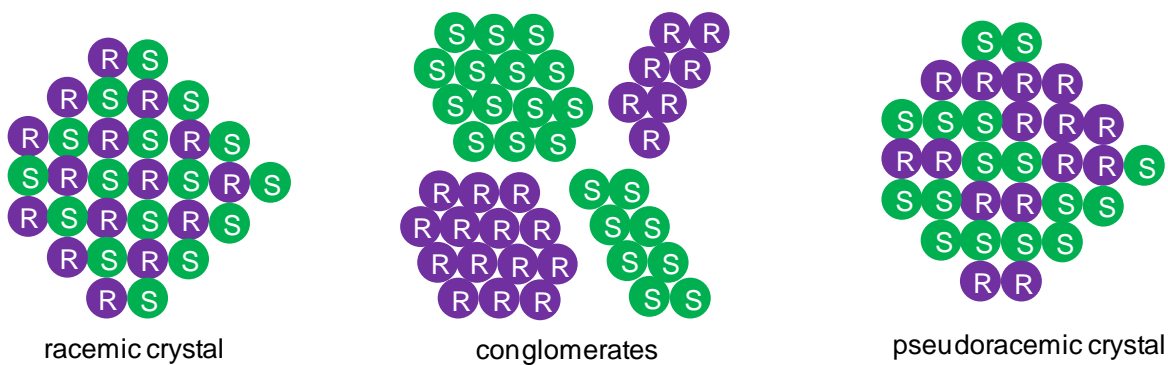
2

Figure 2: The three crystal packing arrangements for chiral compounds.

Research has shown that during heterogeneous nucleation, racemic crystals are the most favorable crystal form under normal conditions. This preference results from more efficient packing of racemates in comparison to pure enantiomers.[4] This observation is known as Wallach's rule, which states that racemic crystals are more stable and denser than chiral crystals.[5] Consequently, inducing racemates in solution to crystallize separately as conglomerates generally is difficult to achieve.

Formation of conglomerates in and of itself does not allow effective purification of enantiomers because equal masses of homochiral R and S crystals form as a mixture. Only in the event that crystals of one enantiomer nucleate and grow selectively in the absence of crystals of the opposite enantiomer does homochiral nucleation allow enantiomers to be separated. *Central to this project is the hypothesis that crystallization of racemates on chiral surfaces not only promotes homochiral nucleation leading to formation of conglomerates, but more importantly, allows selective nucleation of crystals of one enantiomer leading to enantiomeric enrichment.*

3

1.2 Self-Assembled Monolayers

Self-assembled monolayers (SAMs) are ordered molecular assemblies formed by a specific molecule having an affinity for a solid substrate (e.g., precious metals, SiO_2).[6, 7] Molecules that form SAMs typically have three distinct components: a head group, a hydrocarbon tail and a functional group positioned at the end of the tail. The head group consists of a reactive group that binds the molecule to the solid substrate via formation of a covalent bond. The tail acts as a spacer that separates the head group from the functional group. In addition, the tail promotes packing of molecules to form an ordered monolayer on the surface of the substrate such that the functional groups are exposed on the surface of the SAM. The functional group determines the surface interaction energy with molecular species that come in contact when placed on the surface of the SAM. The most widely studied types of SAMs are alkanethiols on gold surfaces.[8, 9, 10, 11] The sulfur atom of the thiol group spontaneously forms a sulfur-gold bond involving reductive elimination of the hydrogen according to the reaction below. Having a hemolytic bond strength of ~44 kcal/mol, this sulfur gold bond is quite strong. [12, 13]

$$RS\text{-}H + Au^0 \longrightarrow RS^-Au^+Au^0 + \tfrac{1}{2} H_2$$
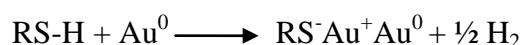
1.2.1 Applications of SAMs

SAMs are used broadly for surfaced applications such as electrochemistry,[14] biosensors,[15] protein separation[16] and enantiomer separation[17] due to the ease with which the surface energy can be tuned based on the choice of functional group. For example, an alkanethiol such as 1-dodecanethiol produces a SAM that is hydrophobic due to the nonpolar methyl groups exposed at the surface. In contrast, a thiol such as 11-mercaptoundecanoic acid produces a SAM that is hydrophilic due to the polar carboxylic acid groups exposed at the surface. Other properties of

SAMs such as the molecular packing arrangement, amount of order/disorder, and film thickness can be adjusted by changing the composition and length of the hydrocarbon tails.

1.2.2 Chiral SAMs

This project focuses on the use of chiral SAMs for enantiomer separation. Chiral SAMs can be produced by reacting gold substrates with thiols that feature chiral groups in the tail or functionality exposed at the terminus of the tail. In order to promote homochiral crystallization of a single enantiomer from a racemic solution, it is vital that the chiral center is exposed on the surface of the SAM. The highly ordered and oriented behavior of the chiral group on the surface of the SAM gives the system a unique advantage when compared to other thin films. [18, 19] The width of the chiral group at the surface of the SAM will play a major role in the effectiveness of the SAM in interacting selectively with a given R or S enantiomer of a drug by forming diastereomeric interactions (e.g., R_{SAM}-S_{drug} vs R_{SAM}-R_{drug} or S_{SAM}-S_{drug}) that promote homochiral aggregation. Previous work in our lab has shown that crystallization of racemic drugs on chiral SAMs of D- or L-cysteine favors homochiral nucleation resulting in enantiomeric enrichment, referred to as enantiomeric excess (ee), as high as 75% (where ee is defined as the difference in the mole fraction of each enantiomer). In the present work, we hypothesized that increasing the size of substituents attached to the chiral centers of cysteine would considerably spread out the molecules in the SAM from one another, thereby magnifying chiral interaction with racemates in solution.

1.3 Chiral Resolution

Development of an effective surfaced-based approach to enantiomer separation will have a significant impact on the development of pharmaceuticals. Many chiral drugs exhibit vastly

different biological effects depending on which enantiomer is used. For instance, one enantiomer may show high therapeutic efficacy. While the other may show reduced or no efficacy, or even an adverse effect. For example, one enantiomer of the drug naproxen treats arthritis pain, while the other causes liver poisoning without providing any beneficial medicinal effect. Therefore, development of new approaches to separate enantiomers in a cost efficient way is a high priority for pharmaceutical companies. Furthermore, in 1992, the US Food and Drug Administration (FDA) permitted the manufacturing and selling of a pure enantiomer of a drug that has already been on the market as a racemic drug.[20] This ruling fueled the desire of pharmaceutical companies to develop new and more effective ways to separate racemates. Currently, the most prevalent techniques used to separate enantiomers are chiral chromatography and the use of chiral resolving reagents. Although both methods are used widely, they often result in poor separation and can add significantly to the cost of marketing drugs.

1.4 Measuring Enantiomer Excess

1.4.1 Differential Scanning Calorimetry

Determining the enantiomeric purity of a crystalline sample is essential for assessing the effectiveness of a chiral SAM toward resolving racemates. The most common method for determining enantiomeric purity is to measure optical rotation using a polarimeter. That technique could not be used for this study because gram quantities of sample are required to accurately determine the ratio of enantiomers present in solution. An alternative method to determine enantiomeric purity that requires milligram quantities of sample is differential scanning calorimetry (DSC). That technique relies on that fact that the melting points and thermal behavior of crystals of a pure enantiomer, a conglomerate, and a racemic crystal differ,

thus allowing the three crystalline forms to be distinguished and identified. DSC also provides a direct measure of the heats of fusion for each form, as well as the temperature range and heat that allow conglomerates, racemic crystals, crystals of pure enantiomers, and mixtures of the three to be identified. In addition to verifying enantiomeric purity, DSC can be used for many different applications, including analysis of polymers[21], oxidative stability[22] and liquid crystals.[23] Although DSC does not determine which enantiomer is in excess, it can be used to find the percent of enantiomeric excess of one enantiomer with respect to the other. It achieves this by analyzing the differing melting points and thermal behavior of a pure enantiomer crystal and a racemic mixture. [24, 25]

In the case of an unequal mixture of crystals of two enantiomers, the enantiomer that is the minor component in the mixture behaves as an impurity that depresses the melting point of the major enantiomer. A typical DSC plot for such a mixture is illustrated in Figure 3. The plot shows two peaks of interest, a eutectic peak at lower temperature and an enantiomer peak at higher temperature. The eutectic peak represents the maximum depression in melting point caused by mixing of equal amounts of crystals of the two enantiomers. . The enantiomer peak signifies the amount of the enantiomer that is in excess.
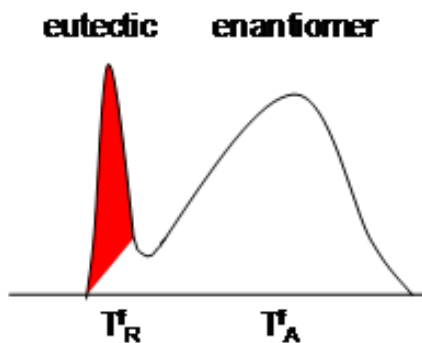

Figure 3: A general heating curve for a chiral compound. The eutectic peak (red) melts at a lower temperature than the pure enantiomer.

1.4.2 Binary Phase Diagrams

Before enantiomeric excess can be measured, a binary phase diagram must be made for the compound in question. A binary phase diagram is a plot of melting data from a series of binary mixtures of two enantiomers varying in mole fraction from 0 to 1. The binary phase diagram for conglomerates differs from that of a racemic crystal as shown in Figure 4.
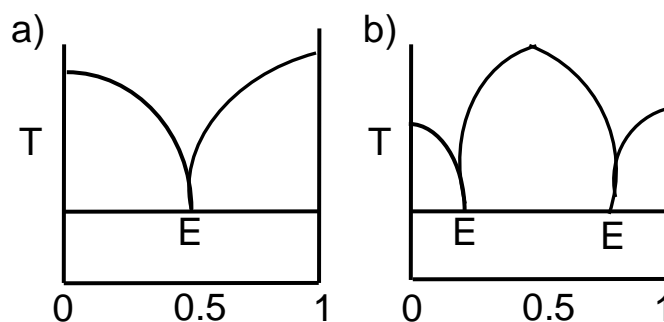

Figure 4: a.) A binary diagram for a compound that forms conglomerates. b.) A binary phase diagram for a compound that forms racemic crystals.

For conglomerates that do not form racemic crystals, the minor enantiomer acts as an impurity to the other and reduces the melting point of the major enantiomer. As shown in Figure 4a, the maximum depression in melting point, referred to as the eutectic, occurs at a mole fraction of 0.5, when equal amounts of crystals of both enantiomers are present.[26] In contrast, binary mixtures that form racemic crystals show a maximum melting point at mole fraction 0.5 due to the greater stability of racemic crystals compared to those of pure enantiomers. Therefore, the eutectic of a racemic crystal is found at a composition below and above the mole fraction where crystals of pure enantiomer behave as impurities. Figure 4b displays a general binary phase diagram for racemic crystals. Once a binary phase diagram is determined, one can compare the temperature at which the excess pure enantiomer melts to the binary phase diagram to determine

the enantiomeric excess in a sample of unknown composition. From knowledge of the enthalpy of fusion of the pure enantiomer and the melting point of the racemate and the pure enantiomer, one can easily calculate the mole fraction of the eutectic present using the Schröder-Van Laar equation shown below.[5, 27]

$$\ln x = \frac{\Delta HA}{R} \left(\frac{1}{TA} - \frac{1}{TR} \right)$$

x = mol fraction

ΔH_A = enthalpy of fusion of pure enantiomer (kJ/mol)

T_A, T_R = melting point of pure enantiomer and racemate respectively (°C)

2. Objectives

2.1 Introduction

We began this project by settling on an appropriate molecule to use when making the SAMs. In addition to a chiral center and a thiol tail, we wanted this molecule to have at least one large bulky group. We believe that surrounding the chiral center with bulky groups may increase the ability of the chiral SAM to preferentially interact with an enantiomer. We decided that N-(tert-butylthiocarbamoyl)-L-cysteine ethyl ester (BTCC) would serve well as a SAM molecule for the above reasons.

Our next step in the project was to pick racemic drugs that would serve as a proof of concept for our SAM. We wanted drugs that were known to form conglomerates. It would also be helpful if a binary phase diagram of the drug was available. Both N-acetylleucine and 3-phenyllactic acid filled this criteria. Previous work in our group has shown that both of these drugs tend to form conglomerates. They also both had a reliable binary phase diagram that we could reference.

From this point we sought to utilize experiments that would not only test the chiral SAM for preferential crystallization of one enantiomer in the presence of the other but also test for favored nucleation of the drug on the surface of the SAM rather than any other surface. A series of drop-wise experiments were used to strictly test the preferential crystallization of enantiomers. In these experiments, crystal growth occurs with respect to the evaporation of the solvent. To test the drugs ability to nucleate on the SAM, we devised a series of submersion experiments. In these experiments, the SAM is submerged in a solution of the racemic drug. Crystal growth can

either occur with respect to the evaporation of the solvent (thermodynamic growth) or the cooling of the solution (kinetic growth).

2.2 N-(tert-butylthiocarbamoyl)-L-cysteine ethyl ester (BTCC)

We chose to investigate using N-(tert-butylthiocarbamoyl)-L-cysteine ethyl ester (BTCC) as the chiral thiol for making SAMs. BTCC has previously been used as a chiral derivatization reagent[28] for carrying out enantioselective separation of racemates on chiral stationary phases.
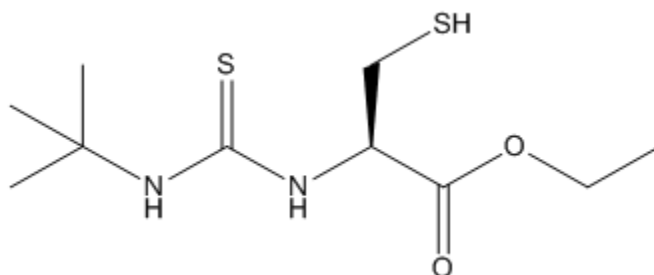
Figure 5: Structure of N-(tert-butylthiocarbamoyl)-L-cysteine ethyl ester (BTCC)

We anticipated that the large t-butyl and ester groups will amplify the chirality (Figure 6) to enhance enantiomeric selectivity during crystallization. The steric bulk of those groups should increase the average diameter of individual thiols molecules such that each chiral center is sufficiently spaced apart on the surface of the SAM ensuring that molecules of the racemic drug can interact with individual chiral centers, and thus increasing the likelihood of chiral discrimination.

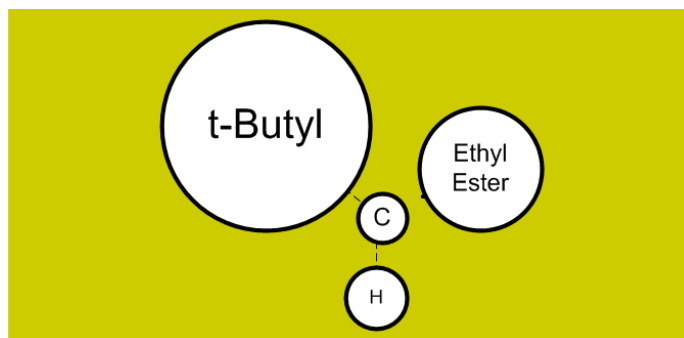**Figure 6: An estimation of how BTCC will align itself on the gold slide. The chiral center is denoted by the letter C.**

Figure 7 shows a pictorial representation of how the BTCC molecules might align within the SAM on the surface of the gold substrate. It is reasonable that the carbonyl of the ethyl ester forms hydrogen bonds with the two thiourea NH donors, as that hydrogen-bonding motif is commonly observed in the crystal structures of ureas. That alignment should expose the substituents on BTCC in the configuration shown in Figure 6.
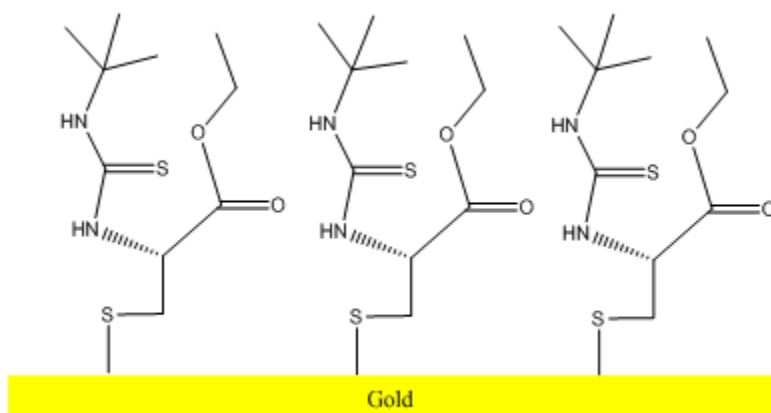

Figure 7: A possible arrangement of the surface of the SAM. Intermolecular hydrogen bonding occurs between the carbonyl of the ester and the two hydrogen atoms of the secondary amines.

2.3 Racemic Drugs

2.3.1 N-Acetylleucine

We chose to investigate crystallization of the racemic N-acetylleucine (NAL) as our test compound for two reasons. We wanted to be able to compare the results of this study to previous results in our group obtained from crystallization of racemic NAL on chiral SAMs of cysteine. In addition, racemic NAL is known to be able to form conglomerates. NAL is an acetyl substituted derivative of the natural amino acid leucine.
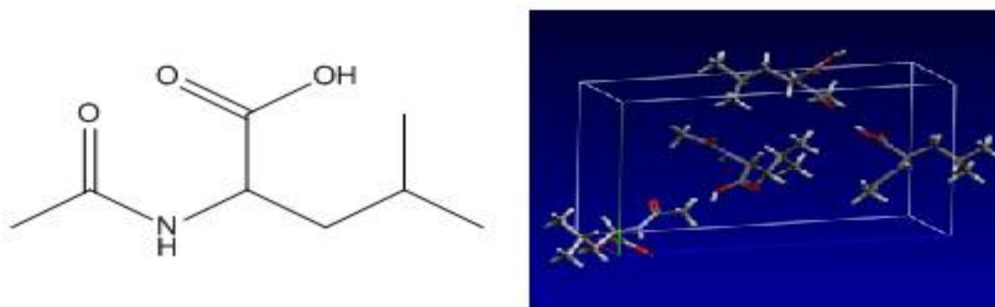
Figure 8 The structure and packing arrangement of N-acetylleucine

NAL is known to promote the growth and repair of muscle tissue.[29] The two acidic hydrogen atoms, one at the carboxylic acid and one at amino group, act as hydrogen-bonding donors. The carbonyl groups of the carboxylic acid and the acetyl group act as hydrogen-bonding acceptors.

The presence of hydrogen-bonding donors and acceptors is important for promoting chiral recognition, aggregation, and nucleation of NAL on the surface of SAMs of BTCC that leads to nucleation on the surface of the SAM as conglomerates rather than racemic crystals. Crystals of the pure enantiomer of NAL melt between 189-191 °C, while a racemic mixture formed by conglomerates melts between 157.8-160 °C.

Figure 9 The binary phase diagram for n-acetylleucine. The 0 value refers to 100% of the D enantiomer and 1 refers to 100% of the L enantiomer.

2.3.2 3-Phenyllactic acid

In addition to N-acetylleucine, crystallization experiments were also conducted using racemic 3-phenyllactic acid (3-PLA). Enantiomeric enrichment of racemic 3-PLA via crystallization on chiral SAMs of cysteine also have been studied previously in our group.
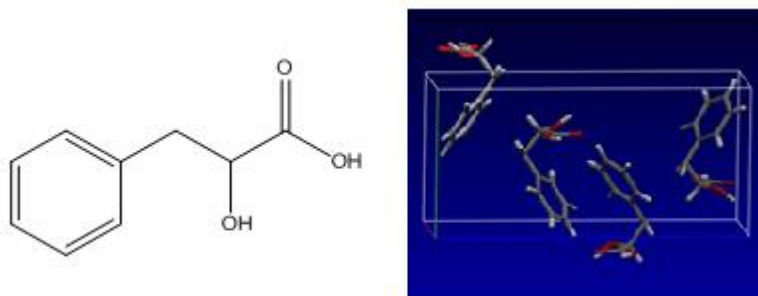
Figure 10 The structure and packing of arrangement of 3-Phenyllactic Acid

3-PLA is a molecular precursor commonly used in the synthesis of various pharmaceuticals. For example, the L-enantiomer is used for the synthesis of chiral intermediates needed for antiviral and antitumor drugs. It has been shown to form conglomerates. The pure enantiomer melts between 95.5-97 °C, while a racemic mixture melts between 124-126.5 °C.
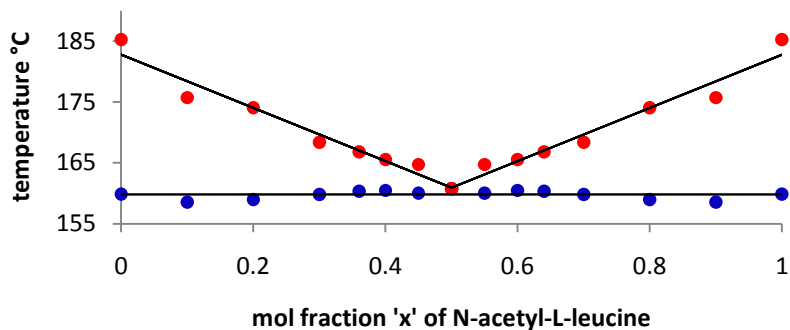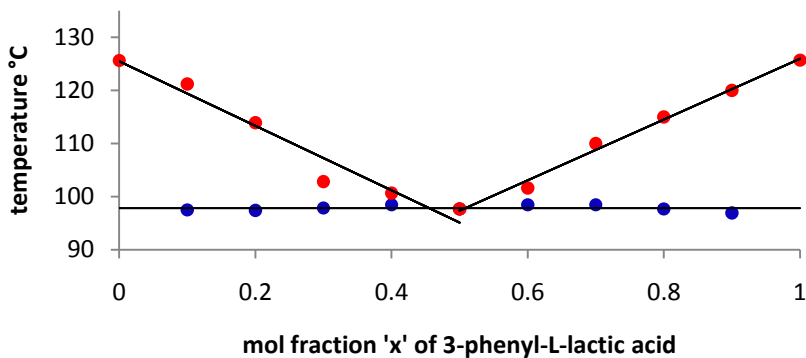

Figure 11 The binary phase diagram for 3-phenyllactic acid. The 0 value refers to 100% of the D enantiomer and 1 refers to 100% of the L enantiomer.

3. Results and Discussion

3.1 Characterization of BTCC SAMs

Contact-angle measurements and grazing angle infrared (IR) spectra were taken to confirm that BTCC had in fact coated the surface of the gold slides. Contact-angle experiments were carried out by placing a 5 µl drop of water on the surface of the SAM and then measuring the angle between the edge of the drop that the surface. Contact-angle measurements provide a relative measure of the wettability of the surface by water that reflects the surface interaction energy at the interface. Water exhibits higher contact angles on nonpolar, hydrophobic surfaces and lower contact angles on polar, hydrophilic surfaces. Grazing-angle IR spectroscopy is sensitive enough to measure the IR absorptions of organic functional groups present in thin molecular films such as SAMs, and was used to confirm the presence of BTCC on the surface of gold substrates.

The contact angles for hydrophobic and hydrophilic control surfaces consisting of SAMs of dodecanthiol and 11-mercaptoundecanoic acid were 107 and 38 degrees, respectively, as shown on the left and right in Figure 12. The contact angle for SAMs of BTCC was 95 degrees (shown in the middle in Figure 12) based on an average of 5 independent measurements, indicating that the SAMs are relatively hydrophobic. The high contact angle corroborates the model for packing of BTCC molecules shown in Figure 7 in which the hydrophilic t-butyl groups are oriented so they are exposed on the surface.
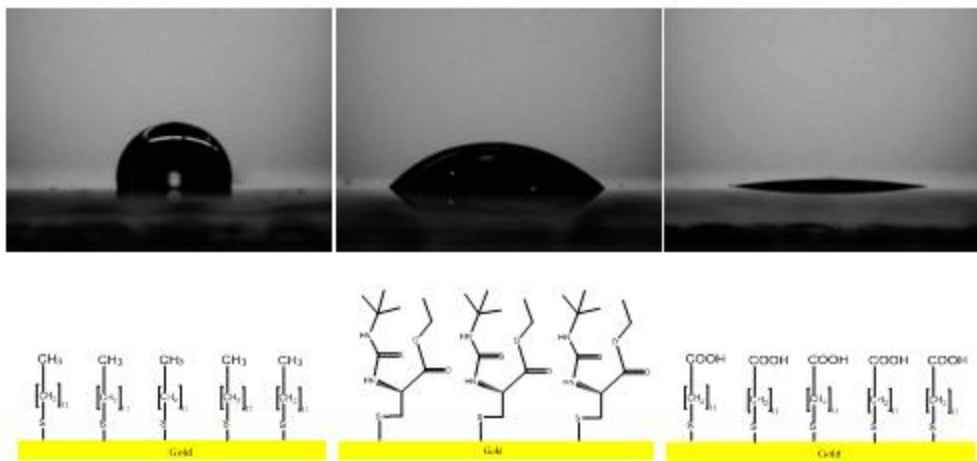
Figure 12 Drops of water on dodecanethiol, BTCC and 11-mercaptoundecanoic acid SAMs (in order from left to right)

The IR spectrum of bulk BTCC and the grazing-angle IR spectrum of SAM of BTCC are shown in Figures 13 and 14, respectively. The grazing-angle IR of the SAM shows bands at 3369, 1265, and 1005 cm^{-1} corresponding to BTCC on the surface. The ester carbonyl stretching band present at 1729 cm^{-1} in the spectrum for bulk BTCC noticeably is absent in the spectrum for the SAM, which suggests the C=O bond of the ester is oriented parallel to the surface of the SAM. Bond dipoles oriented parallel to the surface of gold in SAMs generally are not IR active due to formation of a counter-dipole on the surface of the underlying gold substrate.

Figure 13 The IR spectrum of N-(tert-butylthiocarbamoyl)-L-cysteine ethyl ester

Figure 14 The grazing IR spectrum of an N-(tert-butylthiocarbamoyl)-L-cysteine ethyl ester SAM

3.2 N-Acetylleucine

3.2.1 Crystallization of N-acetylleucine on BTCC SAMs

As described in the experimental section, crystallization of NAL was carried out by applying

drops (~0.5 mL) of a 0.189 M solution of racemic NAL to the surface of five different BTCC

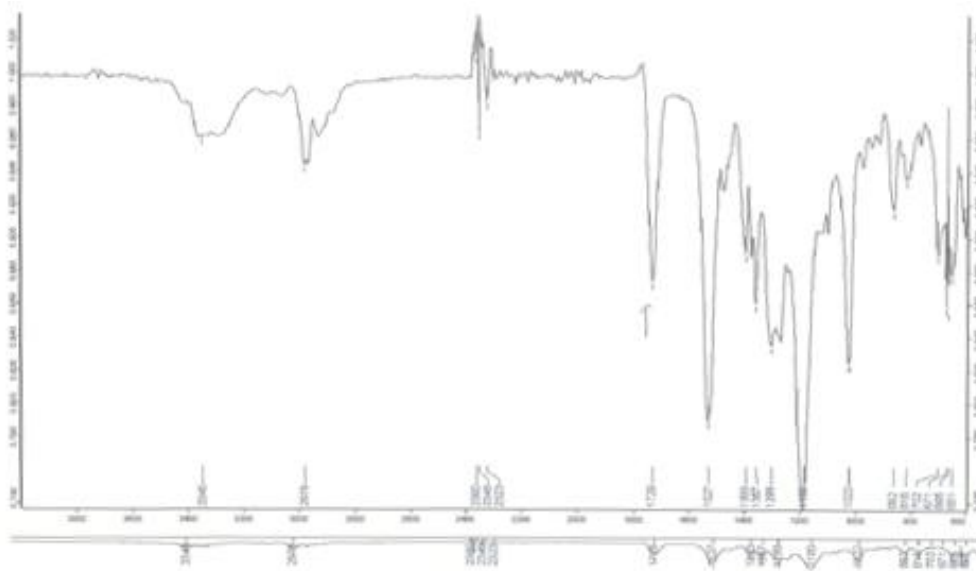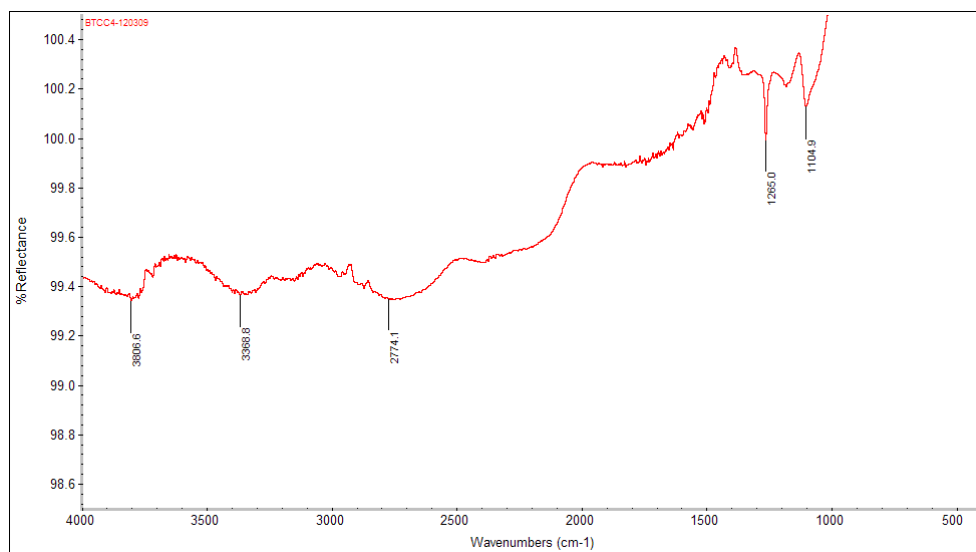SAMs. Two independent sets of five SAMs each yielded crystals in solution on the surface of the

SAMs with rhombus and block morphology. Bulk crystalline samples isolated from the surface

of the SAMs were examined by DSC to determine their composition based on the melting

behavior. All of the DSC plots of racemic NAL crystallized on the BTCC SAMs showed a peak

at temperatures above the eutectic peak indicating an excess of one enantiomer. The eutectic

peak consistently appeared between 159-161°C as expected. Melting data collected from the

first run is shown in Table 1. During the first run, where the bulk samples of crystals were not

ground up, the DSC plots show multiple peaks corresponding to enantiomeric excess (ee) of the

DSC plots between 165-179°C. Comparison of the temperatures of those peaks to the binary

phase diagram of NAL indicates the ee in the samples ranged from 20%-90%. The broad

variability of the ee (e.g., multiple peaks indicating different degrees of enantiomeric excess) of

the samples from the first run can most likely be attributed to the fact that the samples of crystals

were not ground up to form a uniform distribution of crystallites. We hypothesized that large

single crystals of pure enantiomer of different sizes should melt at different rates creating

isolated pockets of pure enantiomer in poor contact with crystals of the opposite enantiomer, thus

resulting in multiple peaks at different temperatures depending on the degree of contamination

by the minor enantiomer leading to melting point depression.

	SAM #	Date	Conglomerate Peak (°C)	Enantiomer Peak (°C)	ee
First Run	1	1/30/2010	160.54	164.24, 169.48, 173.99	0.5-0.2
	2	1/30/2010	160.22	179.23	0.1-0.05
	3	1/30/2010	159.17	167.75, 172.08	0.36-0.2
	4	1/30/2010	159.29	165.47	0.4
	5	1/30/2010	159.55	170.61	0.3-0.2

Table 1 The results of the first run of experiments of crystallization of NAL on BTCC SAMs in a drop-wise fashion.

During the second run, crystallization was carried out identically to the first run. After the

crystals were harvested, the bulk samples were ground up before being placed into the DSC pan.

The second run yielded more consistent melting data when compared to the first run. DSC

melting data collected from the second run is shown in Table 2. Samples 1, 4, and 5 still showed

multiple peaks for indicating variable ee in the same sample ranging from 20% to 60%. This

behavior could be due to the fact that each sample of crystals could not be grounded together

completely. Because only a very small amount of crystals can be recovered from each SAM (1-2

mg), grinding the sample uniformly was generally difficult.

	SAM #	Date	Conglomerate Peak (°C)	Enantiomer Peak (°C)	ee
Second Run	1	3/9/2010	160.02	167.40, 170.41	0.36-0.2
	2	3/9/2010	160.46	168.90	0.3
	3	3/9/2010	160.28	168.50	0.3
	4	3/9/2010	160.23	163.49, 166.02, 169.68	0.5-0.2
	5	3/9/2010	159.92	163.04, 169.72, 172.52	0.5-0.2

Table 2 The results of the second run of experiments of crystallization of NAL on BTCC SAMs in a drop-wise fashion.

From the data in Tables 1 and 2, we concluded that crystallization of racemic NAL on chiral

SAMs of BTCC yield enantiomeric selectivity generally ranging from 60-95% (i.e., 60-95% of

one enantiomer and 5-40% of the other), with an average enantiomeric selectivity of 72%. That

range of selectivity for one enantiomer results in values of ee ranging from 20-90% with an

average ee of 56%. Three of the samples of crystals from runs 1 and 2 showed ee values as high

as 50%, suggesting that SAMs of BTCC are quiet effective in biasing not only formation of

conglomerates over racemic crystals, but more importantly, in biasing crystallization to favor

nucleation and growth of one enantiomer preferentially over the other.

Figures 15 shows the characteristic rhombus and block morphologies of crystals of NAL grown

on BTCC SAMs. The presence of crystals forming along a curve in Figure 15A illustrates the

observed preference crystals to nucleate and grown on the surface of the SAM along the edge of

the receding solution where the concentration of solute is highest due to the gradient in

concentration caused by evaporation of solvent from the surface of the drop. Crystals most

commonly appeared with the rhombus morphology (Figure 15A) with crystals occasionally

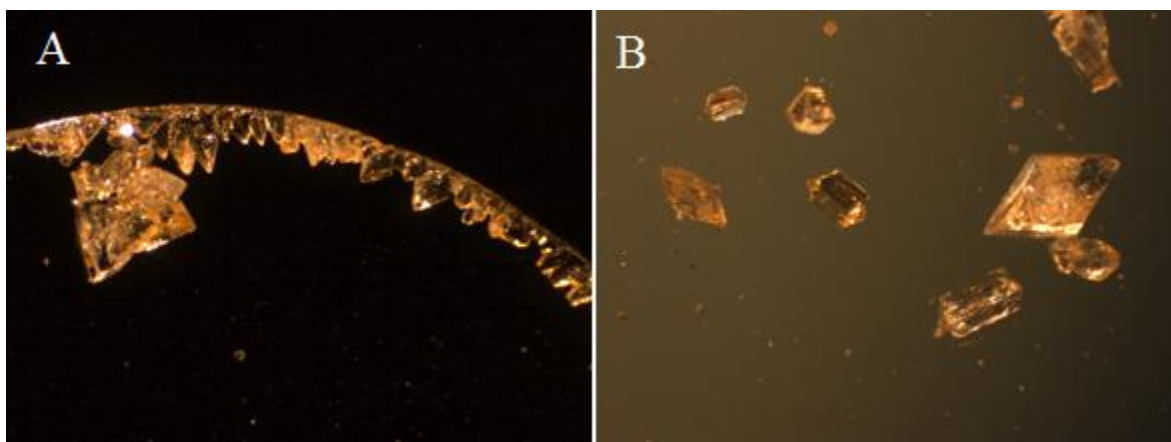appearing with a block morphology, as shown in Figure 15B.

**Figure 15 A.) An image of NAL crystals on a BTCC SAM. The crystals have nucleated along the edge of the water drop.
B.) An image of NAL crystals on a BTCC SAM. Crystals in the shape of both rhombuses and blocks are present and are
in close proximity to one another.**
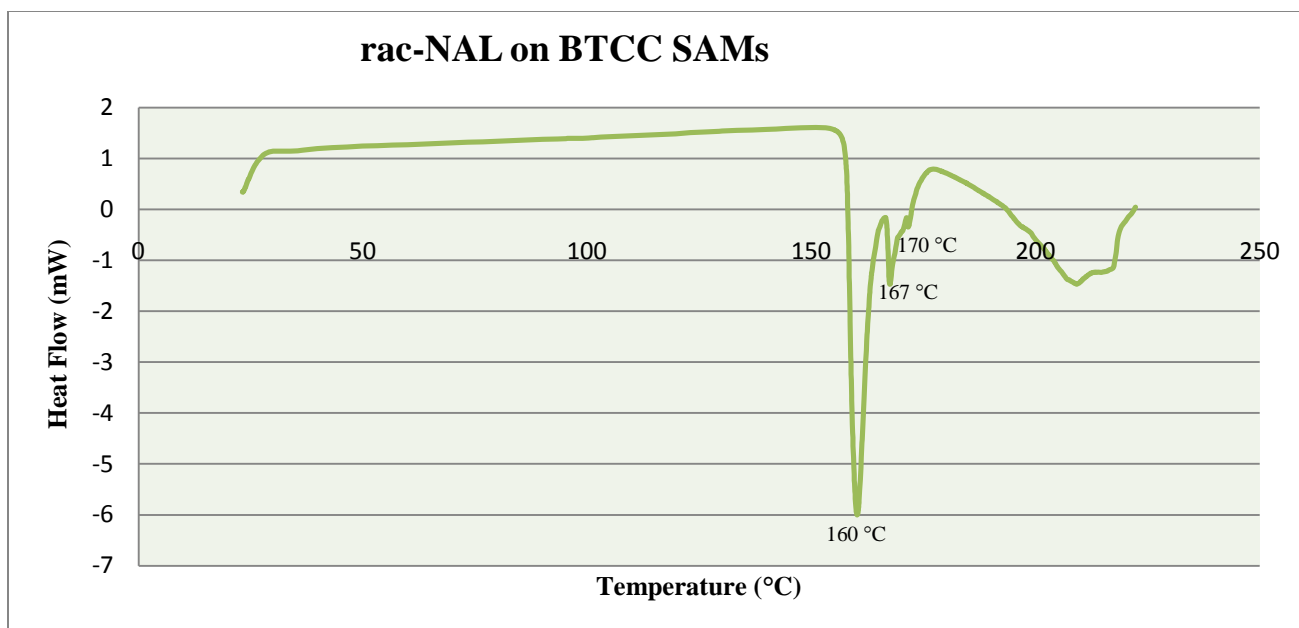
rac-NAL on BTCC SAMs

Figure 16 An example of a DSC plot of NAL on BTCC SAMs. The eutectic peak can be found prominently at 160 degrees. The pure enantiomer peaks can be found between 167-170 degrees.

3.2.2 Thermodynamic Crystallization on BTCC SAMs (Submersion)

The crystallization experiments described above were carried out by placing aqueous solutions onto the surface of horizontal SAMs and then allowing the solution to evaporate. Using that experimental setup, crystals that form necessarily rest on the surface of the SAM regardless of whether they nucleate on the SAM or above the SAM and then fall to the surface. We carried out a different set of crystallization experiments, referred to as submersion experiments, in which SAMs were completely submerged in the growth solutions with the gold slide tilted upward at an angle with the SAM inverted underneath the slide to determine whether crystals nucleate on the surface of the SAM and remain bonded to the SAM through strong interactions with the SAM. Two different of submersion experiments were carried out. In the first (described in this section), a 0.151 M solution of racemic NAL at RT was allowed to evaporate from the vial to promote slow nucleation and growth of crystals on the SAM under thermodynamic conditions. In the

22

second (described in the next section), a warm ~0.4M solution of racemic NAL was allowed to

cool rapidly from 80°C to RT in order to drive crystallization rapidly under kinetic conditions.

Both the thermodynamic and kinetic submersion experiments differ substantially from the drop

experiments. While the drop experiments test the enantiomer preference of the BTCC SAM, the

submersion experiments examine the affinity of crystals of NAL for the surface of the SAM.

Table 3 indicates the locations at which crystals appeared in the vial. Racemic NAL as well as

the L enantiomer were used to analyze if there was a difference in the preferential nucleation

patterns between the two forms.

	Type of slide	Nucleation on surface of SAM	Nucleation on glass top of the slide	Crystals on bottom of glass vial	Crystals floating on top of solution
Racemic NAL	BTCC SAM	None	None	Large crystals	A few small crystals
	BTCC SAM	None	None	Large crystals	None
	Gold	One small crystal	None	Medium crystals	Long, thin crystals
	Glass	None	None	Large crystals	A huge, long crystal
L-NAL	BTCC SAM	None	Medium size crystals	Some medium crystals	A few small crystals
	BTCC SAM	None	Medium size crystals	Some medium crystals	Some medium crystals
	Gold	Medium size crystals	Medium size crystals	Some medium crystals	Some medium crystals
	Glass	None	Medium size crystals	Some medium crystals	Some medium crystals

Table 3: The location of where crystals had and had not formed at the end of a series of thermodynamic crystallization experiments.

We were surprised to find that crystals of NAL did not appear on the surface of the BTCC SAM

under thermodynamic conditions. Crystals did appear on the bottom of the glass vial, on back of

the glass slide supporting the SAM on gold, as well as floating at the meniscus of the solution.

The presence of crystals on the glass top of the slides and floating at the meniscus indicated that those crystals must have nucleated on the glass of the vial or the top of the slide. The crystals on the bottom of the vial could have come from nucleation on the glass at the bottom of the vial, on the glass at the side of the vial, or on the SAM itself. The absence of crystals on the surface of the SAM does not rule out that nucleation may have taken place on the SAM. It does indicate, however, that any crystal nuclei that formed did not adhere strongly enough to prevent gravity from pulling mature crystals off the SAM. The abundance of crystals above and on top of the glass slide indicate that nucleation of NAL on glass competes strongly with nucleation on the BTCC SAM, and may in fact be more favorable due to the ability of NAL to form strong hydrogen-bonding interactions with hydroxyl groups exposed on the surface of glass.

3.2.3 Kinetic Crystallization on BTCC SAMs (Submersion)

Cooling of saturated solutions of racemic NAL resulted initially in formation of crystals along the edge of the meniscus as well and on the bottom of the vial underneath the inverted SAM of BTCC, followed by the appearance of needle-shaped crystals that eventually dropped from the meniscus onto the glass backing of the SAM. At no point did crystals appear on the surface of the inverted SAM. These experiments show that crystals of NAL do not show any preference to bind to BTCC SAMs during kinetic growth. Similar to thermodynamic crystallization by submersion, these experiments suggest that glass competes strongly with the BTCC for nucleation of NAL from solution.

3.3 3-Phenyllactic Acid

3.3.1 Crystallization of 3-Phenyllactic Acid on BTCC SAMs

The crystallization experiments with 3-phenyllactic acid on the BTCC SAMs were much more difficult to extract viable data than those of NAL on the SAMs. 3-phenyllactic appeared to have difficulty in nucleating on the surface of the SAMs. The majority of the runs conducted with 3-PLA in water did not yield any individual crystals. Instead, after approximately two days of evaporation, the clear solutions generally appeared to go almost to dryness and followed by formation of crystalline films on the surface of the SAM within 5 minutes. Analysis of the crystalline films by DSC indicated no enantiomeric excess.
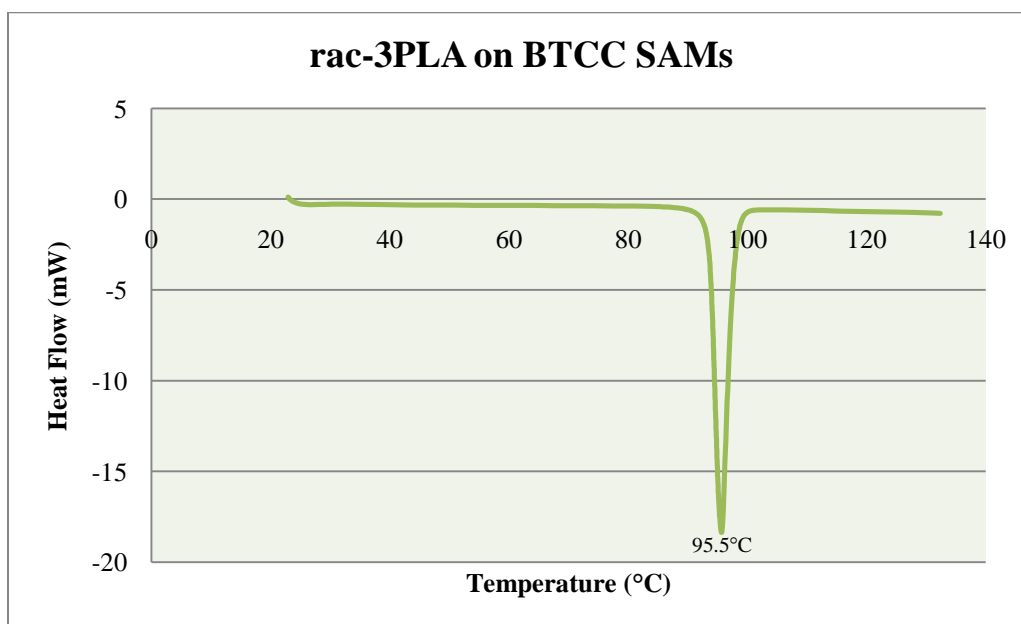

rac-3PLA on BTCC SAMs

Figure 17 An example of a DSC plot of 3-PLA on BTCC SAMs. The eutectic peak can be found prominently at 95.5 degrees.

Crystals rather than crystalline films did form in a few of the runs in a similar fashion to the NAL experiments. The crystals appeared either as long needles or as blocks, as shown in Figure

18. The blocks usually appeared to be twinned with several different crystals growing together. None of the samples of needles or blocks displayed enantiomeric excess when examined by DSC. The DSC traces showed eutectic peaks between 95°C-96.5°C corresponding to racemic mixtures present as conglomerates.
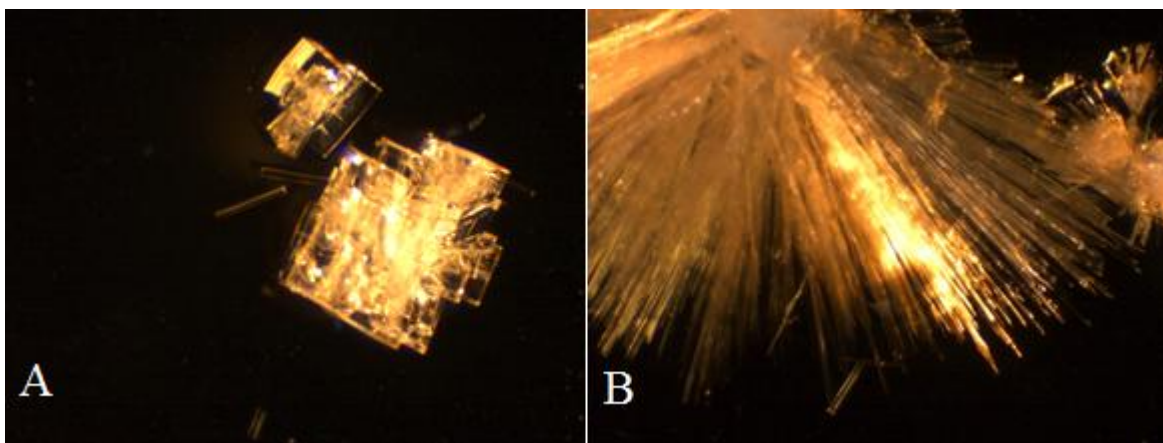

Figure 18 A.) Nucleation of 3-PLA on BTCC SAMs. The twinning nature of the block crystals is quite evident. A few needle-shaped crystals can be seen as well. B.) A image of needle-shaped 3-PLA crystals on BTCC SAMs.

3.4 Difficulties with Crystallization of Compounds on BTCC SAMs

One of the main obstacles when conducting surface chemistry and crystallization experiments is the issue of maintaining an unblemished surface free of defects. Any scratch or nick on the surface serves as a high-energy surface that initiates crystallization. With respect to chiral SAMs, scratching the surface of the SAM may produce an achiral defect that nucleates both enantiomers of a racemate equally. For that reason, care must be taken to avoid scratching the surface, whether it is during the initial cutting of the gold slides, the making of the SAM, or the storing of the SAM.

Figure 19 shows the consequence of using a scratched SAM. In this case, the majority of the

NAL crystals on this SAM originated along the scratch. The resulting crystals lack the typical

shapes associated with NAL crystals (shown towards the top of the photo).
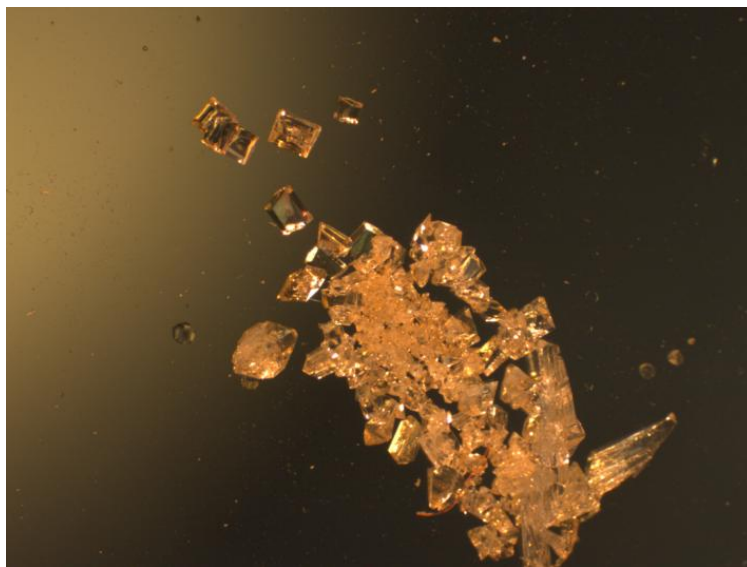

Figure 19 A image of the nucleation of NAL crystal on a small scratch on a BTCC SAM.

Another major obstacle in this project was the lack of nucleation of 3-phenyllactic acid on the

BTCC SAMs. As mentioned previously, 3-PLA usually did not form distinctive crystals on the

surface of the SAM. In an attempt to spur aggregation, the solvent system was changed from

water to 3:1 hexanes/ethyl acetate. Previous work in our group showed that a 3:1 hexanes/ethyl

acetate solvent system, instead of water lead to the formation of 3-PLA crystals on different

types of SAMs. Attempts to grown crystals of 3-PLA on SAMs of BTCC using that solvent

system were, however, unsuccessful in producing significant quantities of crystals. In cases

where crystals did form, DSC analysis showed no enantiomeric enhancement.

4. Experimental

4.1 Synthesis, purification and characterization of N-(tert-butylthiocarbamoyl)-L-cysteine ethyl ester (BTCC)
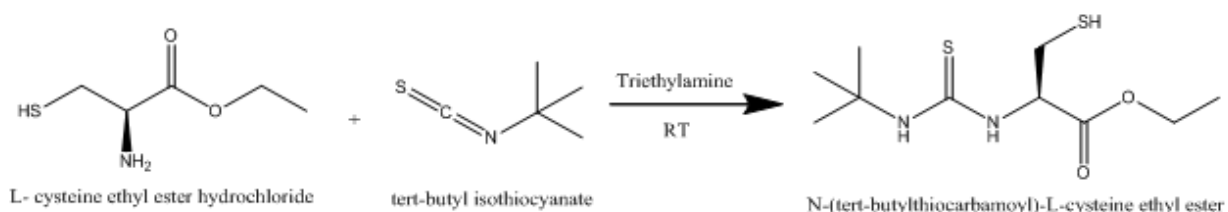

Figure 20: The synthesis of N-(tert-butylthiocarbamoyl)-L-cysteine ethyl ester

100 mol of acetonitrile was added to a flask of 2.33 grams of tert-butyl isothiocyanate. 2.40 grams of triethylamine was then added to the mixture. Lastly, 4.427 grams of L-cysteine ethyl ester hydrochloride was added. The cloudy reaction mixture was allowed to stir at room temperature for 24 hours. After filtration and washing with 1M HCl, 5% NaHCO3 and water, the reaction mixture was reduced to 3.3 grams of a yellow oil. A proton NMR showed an impure product. To purify the product, a column was run in a glass pipet. The solvent system used was 80:1 dichloromethane to methanol. Pure product was collected and analyzed with H^1 NMR, C^{13} NMR, IR and GCMS.

4.2 Preparing of gold and glass slides

The gold slides were purchased from Evaporated Metal Films (EMF). These slides are prepared as followed. A 1 in x 3 in x 0.04 in glass slide is coated with 50 A chromium layer and then a 1000 A thick gold layer. These gold slides, as well as plain glass slides with similar dimensions, are then cut in 1 in x 1 in squares. The surfaces are then cleaned using a plasma oxidizer manufactured by SPI Supplies Plasma-Prep II.

4.3 Making and characterization of BTCC SAMs

Ten gold slides were placed into 50 mL of a 2 mM solution of BTCC in pure ethanol. The slides were left overnight in the solution. In addition, dodecanthiol and 11-mercaptoundecanoic acid SAMs were made to use for comparison purposes. The next day, the slides were taken out of the solution, rinsed with pure ethanol and water, and then dried with nitrogen gas. After being completely dried, the SAMs were placed in a covered Petri dish which was sealed with parafilm.

4.4 Crystallization of N-acetylleucine on BTCC SAMs

A 0.189 M solution of racemic N-acetylleucine in water was made. The solution was heated and stirred vigorously to completely dissolve the compound. 5-10 drops of the solution was put on the BTCC SAMs, as well as, on plain gold slides and glass slides. The above procedure was followed using a 0.137 M solution of N-acetyl-L-leucine in water. The N-acetylleucine solution was left on the BTCC SAMs for roughly 19 hours. Once crystals began to form, the mother liquid was washed off and the crystals were washed with water and dried with nitrogen gas.

4.5 Thermodynamic Crystallization of N-acetylleucine on BTCC SAMs (Submersion)

40 mL of a 0.151M solution of racemic N-acetylleucine in water was heated until all of the NAL was dissolved. The solution was poured into four vials. Two of the vials contained a BTCC SAM. The other two vials contained a gold slide and a glass slide. It is important to note that each slide must be leaning in the vial with the SAM side (or gold side, depending on the vial) facing down towards the bottom of the vial. This is done to test, without a doubt, weather the SAM attracts nucleation of the drug.
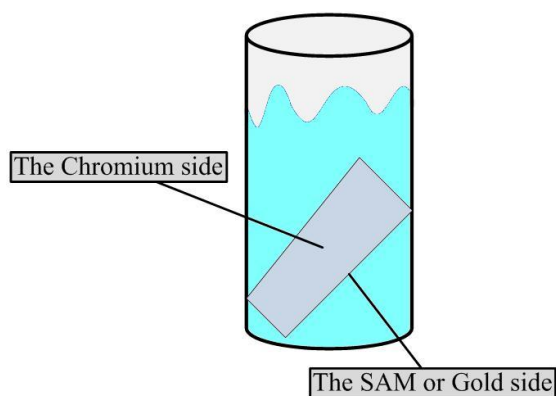
Figure 21: The layout of the set up for the thermodynamic and kinetic experiments. Notice that the SAM side is facing towards the bottom of the vial.

Similarly, a 40 mL of a 0.130M solution of N-acetyl-L-leucine in water was also prepared. Four vials (SAM [2], gold and glass) were also prepared in a similar method to the racemic experiment. After 72 hours had passed, each vial was examined and then the slides were taken out of solution and dried under nitrogen gas.

4.6 Kinetic Crystallization of N-acetylleucine on BTCC SAMs (Submersion)

A vial with 10 mL of a fully saturated solution of racemic N-acetylleucine in water was heated until all of the NAL was dissolved. NAL was added to the solution until the compound would not dissolve anymore. Then, a small amount of water was added to dissolve the remaining amount of NAL. Once fully dissolved, a BTCC SAM, which has heated slightly using the hot plate, was added to the vial and the vial was taken off the hot plate. After 15 minutes, the SAM was taken out of the vial and dried with nitrogen gas.

4.7 Crystallization of 3-Phenyllactic Acid on BTCC SAMs

A 0.3 M solution of racemic 3-phenyllactic acid in water was made. The solution was heated
and stirred vigorously to completely dissolve the compound. 5-10 drops of the solution was put
on the BTCC SAMs. The 3-PLA solution was left on the BTCC SAMs for roughly 35 hours.
On the SAMs that crystal had formed on, the mother liquid was washed off and the crystals were
washed with water and dried with nitrogen gas.

4.8 Characterization of Crystals for Enantiomeric Excess

To characterize our harvested crystals, we mostly used differential scanning calorimetry (DSC).
Once the mother liquid has been poured off the SAM and the crystals have been blown dry with
nitrogen gas, the crystals are scraped off the surface of the SAM on to a sheet of weighing paper.
It is important to collect all the crystals that have grown on the surface of the SAM. This allows
for the DSC plot to give an adequate measure of the enantiomeric excess of the crystals on the
SAM. At this point the crystals are placed on a watch glass. With a spatula, the crystals are
carefully ground up. As explained in a previous section, it is important to not grind the crystals
too much. An aluminum DSC pan is then preweighed. Carefully, the ground up crystals are
poured into this DSC pan and the mass of the crystals is calculated. Hopefully, the mass will be
above 1 mg, which is the cutoff to ensure an accurate DSC run. An aluminum top is then place
on top of the pan and secured. The sealed pan can then be placed into the DSC well. A
reasonable run procedure for NAL and 3-PLA is to equilibrate the instrument at 25 degrees and
then raise the temperature 10 degrees every minute with the run ending at 300 degrees.

5. Conclusion

This project succeeded in showing the effectiveness of SAMs using BTCC monolayers to separate certain chiral compounds. The 72% enantiomeric selectivity (56% ee) of NAL on the SAMs proves the efficacy of this chiral SAM. However, the lack of nucleation on the SAM during the thermodynamic and kinetic submersion experiments limits the practicality of the SAM. Nevertheless, with what has been learned of BTCC SAMs, research of other cysteine derivatives as well as other thiol molecules is inevitable. However, in all likelihood, the transition from gold surfaces to a cheaper surface, such as glass, is a predicable next step. One possible example would be the use of silane head groups, which are known to bind strongly to glass. A molecule that shows a similar enantiomeric selectivity to that of BTCC but also observes nucleation in either (or both) of the submersion experiments would make a suitable candidate for the addition of a silane head group. The research described in this report has succeeded in advancing our group's efforts in developing a new surface-based approach to separating enantiomers of racemic drugs.

6. References

[1] Weissbuch, I.; Addadi, L.; Lahav, M.; Leiserowitz, L. *Science (Washington, DC, United States)* **1991**, *253*, 637-45.

[2] Weissbuch, I.; Lahav, M.; Leiserowitz, L. *Crystal Growth & Design* **2003**, *3*, 125-150.

[3] Lee, A. Y.; Ulman, A.; Myerson, A. S. *Langmuir* **2002**, *18*, 5896-5898.

[4] Brock, C. P.; Schweizer, W. B.; Dunitz, J. D. *J. Am. Chem. Soc.* **1991**, *113*, 9811-9820.

[5] Jacques, J.; Collet, A.; Wilen, S. H. *Enantiomers, Racemates and Resolutions*; John Wiley and Sons: New York, 1981.

[6] Bigelow, W. C.; Pickett, D. L.; Zisman, W. A. *Journal of Colloid Science* **1946**, *1*, 513-38.

[7] Ulman, A. *Chem. Rev.* **1996**, *96*, 1533-1554.

[8] Nuzzo, R. G.; Allara, D. L. *Journal of the American Chemical Society* **1983**, *105*, 4481-3.

[9] Bain, C. D.; Troughton, E. B.; Tao, Y. T.; Evall, J.; Whitesides, G. M.; Nuzzo, R. G. *Journal of the American Chemical Society* **1989**, *111*, 321-35.

[10] Bain, C. D.; Whitesides, G. M. *Journal of the American Chemical Society* **1989**, *111*, 7164-75.

[11] Laibinis, P. E.; Whitesides, G. M.; Allara, D. L.; Tao, Y. T.; Parikh, A. N.; Nuzzo, R. G. *Journal of the American Chemical Society* **1991**, *113*, 7152-67.

[12] Ulman, A. *Chem. Rev.* **1996**, *96*, 1533-1554.

[13] Sellers, H.; Ulman, A.; Shnidman, Y.; Eilers, J. E. *Journal of the American Chemical Society* **1993**, *115*, 9389-401.

[14] Zheng, M.; et al. *Talanta* **2010**, 81, 1076-1080.

[15] Smith; et al. *Progress in Surface Science* **2004**, 75, 1–68.

[16] Chaki, N. K.; Aslam, M.; Sharma, J.; Vijayamohanan. *K. Proc. Indian Acad. Sci.* **2001**, 113, 659–670.

[17] Binnes, R.; Gedanken, A; Margel, S. *Tetrahedron Letters* **1994**, 35, 1285-8.

[18] Nuzzo, R. G.; Allara, D. L. *Journal of the American Chemical Society* **1983**, *105*, 4481-3.

[19] Nuzzo, R. G.; Fusco, F. A.; Allara, D. L. *Journal of the American Chemical Society* **1987**, *109*, 2358-68.

[20] "Development of New Stereoisomeric Drugs." U S Food and Drug Administration, 1 May **1992**. Web. <http://www.fda.gov/Drugs/GuidanceComplianceRegulatoryInformation/Guidances/ucm122883.htm>.

[21] Barton, J. M.; Hamerton, I.; Rose, J. B.; Warner, D. *Polymer.* **1991**, 32, 2482-2490.

[22] Partanen, R. *VTT Technical Research Centre of Finland*. **2008**, 697.

[23] Naslund, R. A.; Jones, P. L. *Ft. Belvoir :Defense Technical Information Center*. **1992**, 9.

[24] Brock, C. P.; Schweizer, W. B.; Dunitz, J. D. *J. Am. Chem. Soc.* **1991**, *113*, 9811-9820.

[25] Jacques, J.; Collet, A.; Wilen, S. H. *Enantiomers, Racemates and Resolutions*; John Wiley and Sons: New York, **1981**.

[26] Brock, C. P.; Schweizer, W. B.; Dunitz, J. D. *J. Am. Chem. Soc.* **1991**, *113*, 9811-9820.

[27] Collet, A.; Brienne, M. J.; Jacques, J. *Chem. Rev.* **1980**, *80*, 215-230.

[28] Nimura, N.; Fujiwara, T.; Watanabe, A.; Sekine, M.; Furuchi, T.; Yohda, M.; Yamagishi, A.; Oshima, T.; Homma, H. *Analytical Biochemistry* **2003,** 315, 262–269

[29] Combaret, L.; Dardevet, D.; Rieu, I.; Pouch, M.-N.; Bechet, D.; Taillandier, D.; Grizard, J.; Attaix, D. *Journal of Physiology (Oxford, United Kingdom)* **2005**, *569*, 489-499.